

Blurring-Invariant Riemannian Metrics for Comparing Signals and Images

Zhengwu Zhang, Eric Klassen, Anuj Srivastava
Florida State University

zhengwu, anuj@stat.fsu.edu
klassen@math.fsu.edu

Pavan Turaga, Rama Chellappa
University of Maryland

pturaga, rama@umiacs.umd.edu

Abstract

We propose a novel Riemannian framework for comparing signals and images in a manner that is invariant to their levels of blur. This framework uses a log-Fourier representation of signals/images in which the set of all possible Gaussian blurs of a signal, i.e. its orbits under semigroup action of Gaussian blur functions, is a straight line. Using a set of Riemannian metrics under which the group actions are by isometries, the orbits are compared via distances between orbits. We demonstrate this framework using a number of experimental results involving 1D signals and 2D images.

1. Introduction

Blurring is omnipresent in image data. The point spread function of the imaging device introduces some level of blurring in the captured images which can be further exaggerated due to techniques for storage and processing. Standard metrics for image comparisons provide results that are affected by the amount of blurring present in images. Shown in Fig. 1 are two examples of natural images (top) and their blurred versions (bottom). It has been one of long-standing problems in image analysis to analyze, compare, and evaluate images without the effect of blurring on them.

A common solution has been to *deblur* the images using one of the many techniques available for deblurring [1, 3, 6, 7, 4, 8] and then compare the deblurred images. The problem with this approach is that deblurring is a difficult operation, at least relative to blurring. Secondly, one has to estimate the amount of blurring in images and then try to deblur them using that level. The amount of blur present in an image has been difficult to quantify and estimate in a principled way [5]. For example, the two images in Fig. 1 bottom row have different levels of blurring but it is difficult to quantify that without knowing the original blur parameters. Therefore, in a deblurring approach, one is left with an unresolved issue of amount of deblurring required. Another approach is to define a set of features that are invariant to

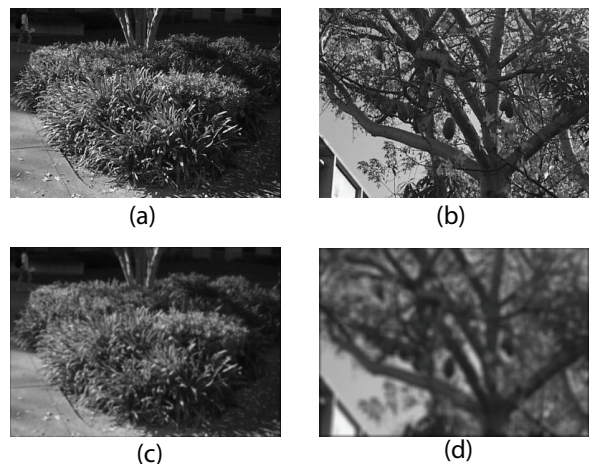


Figure 1. Example of Original (top) and blurred (bottom) images.

blurring and then to compare those features [2]. Usually, these features contain only a limited information about the image and, at best, is a partial representation.

In this conceptual paper, we propose a different approach. Instead of seeking to deblur the images, we propose a metric where a comparison between images is invariant to their level of blurring. If successful, this framework has a large potential of avoiding many computational and theoretical issues associated with deblurring-based solutions. We view the proposed framework as an initial step in that direction, rather than a complete solution to the blurring/deblurring image analysis. The precise goal of this paper is to *develop novel mathematical representations of signal/image data and associated Riemannian metrics such that the resulting image comparisons become invariant to blurring*. To simplify the presentation, we start the discussion with 1D signals, and extend the ideas to 2D or nD signals later.

An important question in developing this framework is: What mathematical form should the signals take? The choice of representations and the metrics should be such that the blurring of any two functions does not change the

distance between them. That is, the action of the blurring group should be by isometries. A natural mathematical representation of a gray-scale image or a signal is simply as a real-valued function on an appropriate domain. We will consider them as real-value functions on \mathbb{R} . (The domain is chosen to be \mathbb{R} since we can easily extend any signal on an interval, say $[0, 1]$, as a periodic signal on the full real line.) Traditionally analysis of signals is performed in the original time (spatial) domain or the frequency domain using Fourier transforms. However, under the commonly used metrics, the action of the (Gaussian) blurring group is not by isometries. In contrast, in the log-Fourier space, the orbits of the blurring group are given by straight lines and the action is by isometries. So, we formulate a framework for blurring-invariant comparisons of signals and images under their log-Fourier representations. We suggest a set of Riemannian metrics in that representation and derive a framework for computing geodesics and geodesic distances between orbits of given signals.

The rest of the paper is as Section 2 introduces the log-Euclidean representation of signals, Section 3 presents the overall algorithm for comparing and matching signals, and Section 4 presents some experimental results to demonstrate the algorithm.

2. Mathematical Representations of Signals

There are at least three different domains one can use to analyze signals – the original space, the Fourier transform space, and the log-Fourier transform space. These three domains and their properties are described next.

1. Time Domain: Let \mathcal{F} be the set of smooth functions $f : \mathbb{R} \rightarrow \mathbb{R}$. (While we shall start with real valued functions, it will become convenient to enlarge our set to the set of complex valued functions.) Let K_δ be a Gaussian blurring function given by $K_\delta(x) = \frac{1}{\sqrt{\delta}} e^{-\pi x^2/\delta}$. The K_δ 's are normalized so that $\int_{\mathbb{R}} K_\delta(x) dx = 1$ for all δ . Let $*$ denote the convolution operation, i.e. $(f * g)(x) = \int_{-\infty}^{\infty} f(y)g(x-y)dy$. It is easy to verify that: $(K_{\delta_1} * K_{\delta_2})(x) = K_{\delta_1 + \delta_2}(x)$. Hence, under convolution, these Gaussians form a semigroup isomorphic to the positive real numbers under addition, which we henceforth denote by \mathbb{R}_+ . Further, the group \mathbb{R}_+ acts on \mathcal{F} by the action:

$$(\delta, f) = (K_\delta * f)(x) = \int_{-\infty}^{\infty} f(y)K_\delta(x-y)dy.$$

This action is nothing but a blurring of the function f by the Gaussian blurring function K_δ . The orbit of a point $f \in \mathcal{F}$ under \mathbb{R}_+ is given by: $[f] = \{(\delta, f) | \delta \in \mathbb{R}_+\}$. In these terms, the problem of interest in this paper is the following. We would like to understand the nature of the quotient space $\mathcal{I} \equiv \mathcal{F}/\mathbb{R}_+$, put a Riemannian metric on it, and calculate geodesics with respect to that metric.

The challenge comes from the fact that the simple \mathbb{L}^2 metric is not invariant to the action of the blurring group. Since \mathcal{F} is a vector space, its tangent space at any point f is also \mathcal{F} . The action of \mathbb{R}_+ on the tangent vectors is same as that on element of \mathcal{F} . Let $\|\cdot\|$ denote the \mathbb{L}^2 metric on \mathcal{F} : for v_1, v_2 , $\langle v_1, v_2 \rangle = \int_{-\infty}^{\infty} v_1(x)v_2(x) dx$. The problem in using this metric for comparing functions is that the action of \mathbb{R}_+ on \mathcal{F} is not by isometry. That is, in general, $\langle v_1, v_2 \rangle \neq \langle K_\delta * v_1, K_\delta * v_2 \rangle$.

2. Fourier Domain: It is often convenient to perform analysis in the Fourier domain since the convolution and deconvolution operations are replaced by more convenient product and division operations. For a $f \in \mathcal{F}$, denote \hat{f} to be the Fourier transform of f : $\hat{f}(\xi) = \int_{-\infty}^{\infty} f(x)e^{-2\pi i x \xi} dx$. The Fourier transform of a blurring function K_δ is given by:

$$\hat{K}_\delta(\xi) = \frac{1}{\sqrt{\delta}} \int_{-\infty}^{\infty} e^{-\pi x^2/\delta} e^{-ix\xi} dx = \frac{1}{\sqrt{\delta}} K_{\delta^{-1}}(\xi).$$

In terms of the Fourier transforms, the convolution becomes a product: $\widehat{f * g} = \hat{f} \cdot \hat{g}$. Let $\hat{\mathcal{F}}$ denote the space of functions (of ξ) obtained as Fourier transforms of functions in \mathcal{F} . Note that these functions can have complex values. The action of \mathbb{R}_+ on $\hat{\mathcal{F}}$ corresponding to the above action on \mathcal{F} is given by $(\delta, \hat{f}) \mapsto \hat{K}_\delta \cdot \hat{f}$. The orbit of a point $\hat{f} \in \hat{\mathcal{F}}$ under \mathbb{R}_+ is given by: $[f] = \{(\delta, \hat{f}) | \delta \in \mathbb{R}_+\}$, and the corresponding quotient space is now given by: $\hat{\mathcal{I}} \equiv \hat{\mathcal{F}}/\mathbb{R}_+$. If we assume the standard \mathbb{L}^2 metric on $\hat{\mathcal{F}}$, once again the action of \mathbb{R}_+ on $\hat{\mathcal{F}}$ is not by isometries.

3. Log-Fourier Domain: We now define a new set of functions from \mathbb{R} to \mathbb{C} , called $\tilde{\mathcal{F}}$, that will provide a convenient domain for our blurring-invariant signal analysis. For a $\hat{f} \in \hat{\mathcal{F}}$, define \tilde{f} such that $\hat{f} = e^{\tilde{f}}$. Let $\tilde{\mathcal{F}} = \{\tilde{f} | e^{\tilde{f}} \in \hat{\mathcal{F}}\}$. Using this transformation, the action of \mathbb{R}_+ acts on $\tilde{\mathcal{F}}$ is given by:

$$(\delta, \tilde{f})(\xi) = \tilde{f}(\xi) - \pi\delta\xi^2.$$

Fig. 2 shows two examples of 1D signals and their log-Fourier transforms (real components) before and after some blurring. These results are based on computer implementations rather than the theoretical expressions and demonstrate an important limitation of the log-Fourier based analysis. Theoretically, the log-Fourier function for the blurred signal is shifted by $-\pi\delta\xi^2$ and the amount of shift should increase as $|\xi|^2$. However, in practice, it follows a parabola until $|\xi| \sim 10$ (for $\delta = 1$) and levels out beyond that. This is because of the limited machine precision in computing the log-Fourier transform of a blurred function beyond $|\xi| > 10$.

The orbit of a point $\tilde{f} \in \tilde{\mathcal{F}}$ under \mathbb{R}_+ is given by: $[f] = \{(\delta, \tilde{f}) | \delta \in \mathbb{R}_+\}$, and the corresponding quotient space is now given by: $\tilde{\mathcal{I}} \equiv \tilde{\mathcal{F}}/\mathbb{R}_+$. In this representation, the orbits are simply straight lines! This is depicted in Fig. 3.

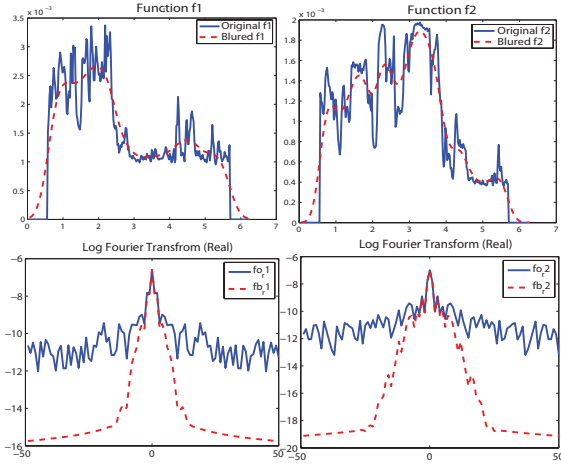


Figure 2. Gaussian blurring of 1D signals and the corresponding effects on their log-Fourier transforms with $\delta = 0.01$ (left) and $\delta = 0.005$ (right).

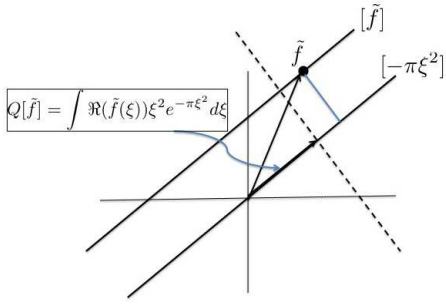


Figure 3. Orbits in the log-Fourier domains and the section perpendicular to the orbits.

Theorem 1 For functions $f, g \in \mathcal{F}$, let f can be written as $f = K_{\delta_0} * g = (\delta_0, g)$, for some $\delta_0 > 0$. Let \hat{f} denote its Fourier transform and \tilde{f} denote the natural log of \hat{f} . Then,

1. The tangent space $T_f([f])$, is a one-dimensional space spanned by the function \hat{f} .
2. The tangent space $T_{\tilde{f}}([\tilde{f}])$, is a one-dimensional space spanned by the function $\xi^2 \hat{f}(\xi)$.
3. In the log-Fourier domain, we already know that the orbits are straight lines. Hence, the tangent space $T_{\tilde{f}}([\tilde{f}])$, is also a straight line $\{\delta \xi^2 | \delta \in \mathbb{R}\}$.

Proof: It is easy to calculate the tangent vector of an \mathbb{R}_+ orbit in $\tilde{\mathcal{F}}$ passing through \tilde{f} as follows. Express \tilde{f} as an element of an orbit by $\tilde{f}(\xi) = e^{-\pi \delta_0 \xi^2} \hat{g}(\xi)$. Then, the tangent vector to this orbit at \tilde{f} is given by:

$$\frac{d}{d\delta} e^{-\pi \delta \xi^2} \hat{g}(\xi) |_{\delta=\delta_0} = -\pi \xi^2 e^{-\pi \delta_0 \xi^2} \hat{g}(\xi) |_{\delta=\delta_0} = -\pi \xi^2 \tilde{f}(\xi).$$

Thus, the tangent vector to the \mathbb{R}_+ -orbit through \tilde{f} is simply spanned by the function $\xi^2 \tilde{f}(\xi)$. Because multiplying the Fourier transform by ξ corresponds to operating on f by $\frac{1}{2\pi i} \frac{d}{dx}$, it follows that the tangent to the orbit $[f]$ at f is $Z(\frac{d^2}{dx^2})f(x)$, where Z is a constant. \square

This result says that the flattening of f , achieved by convolving it with Gaussians is, to first order, the same flattening that is achieved by changing f by a small multiple of its own second derivative, i.e., pulling it down where it is concave down, and pulling it up where it is concave up.

There are some practical issues in defining natural log, e.g. $\log(0)$ and the non-uniqueness of the log of a complex number, we take care of using numerical procedures.

3. Blurring-Invariant Metrics

One of our main objectives is to define a metric on the image space that is invariant to the action of \mathbb{R}_+ on \mathcal{F} . We will accomplish this using the transformations to the Fourier and the log-Fourier domains. More specifically, we will impose a Riemannian metric on the log-Fourier domain $\tilde{\mathcal{F}}$ and induce this metric on the spaces $\hat{\mathcal{F}}$ and \mathcal{F} using appropriate mappings.

Let us start by defining a Riemannian metric on $\tilde{\mathcal{F}}$. For any $\tilde{f} \in \tilde{\mathcal{F}}$, let \tilde{v}_1, \tilde{v}_2 be any two tangent vectors. There are at least two possibilities for choosing a metric.

1. **Exponential Riemannian Metric:** Define the metric:

$$\langle \langle \tilde{v}_1, \tilde{v}_2 \rangle \rangle_{\tilde{f}} = \Re \left(\int_{\mathbb{R}} \tilde{v}_1(\xi) \tilde{v}_2(\xi)^\dagger e^{-\pi \xi^2} d\xi \right). \quad (1)$$

Here \dagger denotes the complex conjugate and \Re denotes the real part of the argument.

2. **Polynomial Riemannian Metric:** For $\beta \geq 4$ define the metric:

$$\langle \langle \tilde{v}_1, \tilde{v}_2 \rangle \rangle_{\tilde{f}} = \Re \left(\int_{\mathbb{R}} \tilde{v}_1(\xi) \tilde{v}_2(\xi)^\dagger \frac{1}{(1 + |\xi|)^\beta} d\xi \right). \quad (2)$$

Theorem 2 The action of \mathbb{R}_+ on $\tilde{\mathcal{F}}$ is by isometries with respect to either of these metrics.

Proof: Since the action of \mathbb{R}_+ on $\tilde{\mathcal{F}}$ is just by translation, the action on the tangent space is just by the identity map. So, the inner-products before and after the action remains same. \square

The invariance of the Riemannian metric implies preservation of distances. Take two functions, f_1 and f_2 with log-Fourier transforms \tilde{f}_1 and \tilde{f}_2 , respectively. The distance between them is:

$$\|\tilde{f}_1 - \tilde{f}_2\| = \sqrt{\langle \langle \tilde{f}_1 - \tilde{f}_2, \tilde{f}_1 - \tilde{f}_2 \rangle \rangle}.$$

For a given δ_0 in \mathbb{R}_+ , let $f'_1 = f_1 * K_{\delta_0}$ and $f'_2 = f_2 * K_{\delta_0}$, and their log-Fourier representations $f'_1 = \tilde{f}_1 - \delta_0 \pi \xi^2$ and $\tilde{f}'_2 = \tilde{f}_2 - \delta_0 \pi \xi^2$. The distance between these two new functions remains same:

$$\|\tilde{f}'_1 - \tilde{f}'_2\| = \|(\tilde{f}_1 - \delta_0 \pi \xi^2) - (\tilde{f}_2 - \delta_0 \pi \xi^2)\| = \|\tilde{f}_1 - \tilde{f}_2\|.$$

It can be shown that with this metric $\tilde{\mathcal{F}}$ is a Hilbert space and the geodesics in this space are simply the straight lines. Since the group action is by isometries, the metric descends to the quotient space $\tilde{\mathcal{F}}/\mathbb{R}_+$ and one can define the distance between the blur orbits as:

Definition 1 The blur-invariant distance between any two signals f_1 and f_2 is given by:

$$d([f_1], [f_2]) = \min_{\delta \in \mathbb{R}_+} \|\tilde{f}_1 - \tilde{f}_2 - \pi \delta \xi^2\|,$$

where the norm is computed using one of the two possible metrics.

3.1. Quantification of Blurring

In order to characterize the quotient space $\tilde{\mathcal{F}}/\mathbb{R}_+$, we seek a set that is orthogonal to every orbit it meets under the specified metric (also known as an *orthogonal section*). This is easy to do in the log-Fourier space since the orbits are straight lines. Thus, we can easily derive a functional, say Q , on $\tilde{\mathcal{F}}$ whose level sets are orthogonal sections. Such a Q will have the property that its gradient at any point will be tangent to the orbit of \mathbb{R}_+ passing through that point. Let \mathbf{h} be the unit vector in the direction of $\pi \xi^2$.

1. For the exponential metric, it is given by:

$$\mathbf{h} = \frac{-\pi \xi^2}{\sqrt{\langle \pi \xi^2, \pi \xi^2 \rangle}} = \frac{-\xi^2}{\sqrt{\int \xi^4 e^{-\pi \xi^2} d\xi}} = -\frac{2\pi}{\sqrt{3}} \xi^2.$$

Here we have used $\int \xi^4 e^{-\xi^2/2\sigma^2} d\xi = \frac{3}{4\pi^2}$.

2. For the polynomial metric, it is given by:

$$\mathbf{h} = \frac{-\pi \xi^2}{\sqrt{\langle \pi \xi^2, \pi \xi^2 \rangle}} = \frac{-\xi^2}{\sqrt{\int \xi^4 \left(\frac{1}{1+|\xi|}\right)^\beta d\xi}} = \frac{-\xi^2}{\mathcal{C}},$$

where $\mathcal{C} = \sqrt{-2\left(\frac{1}{5-\beta} - \frac{4}{4-\beta} + \frac{6}{3-\beta} - \frac{4}{2-\beta} + \frac{1}{1-\beta}\right)}$.

Theorem 3 The functional $Q : \tilde{\mathcal{F}} \rightarrow \mathbb{R}_+$ such that the gradient of Q at a point \tilde{f} is tangent to the orbit of \mathbb{R}_+ passing through \tilde{f} is given by: $Q[\tilde{f}] = \langle \tilde{f}, \mathbf{h} \rangle$.

Note that for the exponential metric: $Q[-\pi \xi^2] = \frac{2\pi^2}{\sqrt{3}} \int_{\mathbb{R}} \xi^4 e^{-\pi \xi^2} d\xi = \frac{\sqrt{3}}{2}$ and for the polynomial metric: $Q[-\pi \xi^2] = \frac{\pi}{\mathcal{C}} \int_{\mathbb{R}} \frac{\xi^4}{(1+|\xi|)^\beta} d\xi = \pi \mathcal{C}$.

The Q functional can be viewed as a quantification of the level of “blurriness” of a signal f . As we blur a signal using a Gaussian kernel, the corresponding Q value of its representative in the log-Fourier space increases. Since we are going to compute geodesics between any two signals in the quotient space $\tilde{\mathcal{T}}$, we need to bring these images to the same level set of Q using the action of \mathbb{R}_+ , according to Definition 1. As we traverse the orbit of \tilde{f} by adding positive multiples of $-\pi \xi^2$, we need to find a $\hat{\delta}$ such that: $Q[\tilde{f} - \hat{\delta} \pi \xi^2] = c$, where $c > Q[\tilde{f}]$ is the blur level that we want to reach. This implies that $Q[\tilde{f}] + \hat{\delta} Q[-\pi \xi^2] = c$.

1. For the exponential metric: $Q[\tilde{f}] + \hat{\delta} \frac{\sqrt{3}}{2} = c$. Therefore, to bring \tilde{f} to the c level curve of Q , we need $\hat{\delta}$ to be: $\hat{\delta} = \frac{2}{\sqrt{3}}(c - Q[\tilde{f}])$.
2. For the polynomial metric, $Q[\tilde{f}] + \hat{\delta} \pi \mathcal{C} = c$. So $\hat{\delta}$ should be: $\hat{\delta} = \frac{c - Q[\tilde{f}]}{\pi \mathcal{C}}$.

3.2. Algorithm

Given any two signals f_1 and f_2 , the following steps define an algorithm to compute a geodesic path between them in \mathcal{F} , with respect to the induced metric. One can choose either the polynomial or the exponential metric for this algorithm.

1. Normalize f_1 and f_2 and compute the Fourier transforms resulting in \hat{f}_1 and \hat{f}_2 , respectively.
2. Take the natural logarithms resulting in $\tilde{f}_1 = \log(\hat{f}_1)$ and $\tilde{f}_2 = \log(\hat{f}_2)$.
3. Compute the $c_1 = Q[f_1]$ and $c_2 = Q[f_2]$ and let $c_2 > c_1$ WLOG.
4. **Distance:** Find a $\hat{\delta}$ such that $Q[\tilde{f}_1 - \pi \hat{\delta} \xi^2]$ equals c_2 . This is same as blurring the signal f_1 so that the blurriness of the two signals are now same. The distance between the two signal orbits is given by $\|\tilde{f}_1 - \pi \hat{\delta} \xi^2 - \tilde{f}_2\|$, under the chosen metric.
5. **Geodesics:** Compute a straight line between $\tilde{f}_1 - \pi \hat{\delta} \xi^2$ and \tilde{f}_2 and sample it at τ values between 0 and 1:

$$\Psi(\tau) = \tau(\tilde{f}_1 - \pi \hat{\delta} \xi^2) + (1 - \tau)\tilde{f}_2.$$

Map each of these points back into the time domain by first taking their exponential and then computing their inverse Fourier transforms.

4. Experimental Results

In this section we describe some experimental results of the proposed framework.

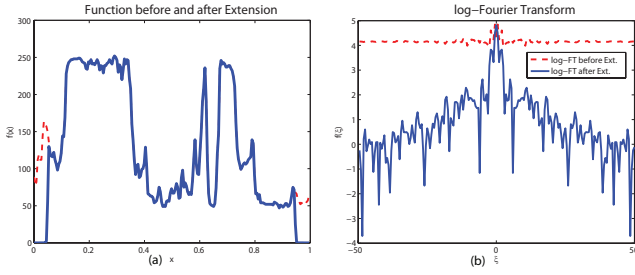


Figure 4. Example of before and after extension of the function

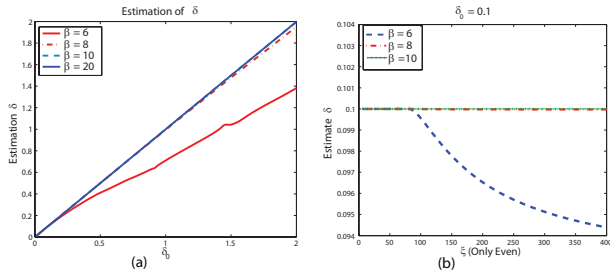


Figure 5. Effect of parameters in the metric. (a) The estimation of $\hat{\delta}$ versus true blurred δ with different β . (b) The estimation of $\hat{\delta}$ versus the frequency domain ξ .

1D Signal Comparisons: The signals used in these experiments are taken from randomly selected rows of some natural images. In order to convert a signal on an interval, say $[0, 1]$ into a smooth periodic signal by repetition, we first decay the signal to a zero value in a smooth fashion in a small neighborhood on 0 and 1, say $(0, r)$ and $(1 - r, 1)$. In the experiment we multiply a factor $\frac{e^{(-1/x)}}{e^{(-1/x)} + e^{(1/(r-x))}}$ to the signal in the small neighborhood. This is shown in Fig. 4 where we show a signal before and after this zeroing of its tail. As can be seen in the right panel, the corresponding effect on its log-Fourier function is quite significant.

In the first set of results, we take a signal f_1 and generate f_2 by blurring f_1 by K_{δ_0} for a certain $\delta_0 > 0$. Since both the functions belong to the same orbit, we expect the blurring-invariant distance between them to be zero. As described in the Steps 3-4 of the Algorithm, we estimate the blur level by comparing the Q -values of the two signals and estimate $\hat{\delta}$ so that the two signals are at the same Q -level. Ideally, one expects $\hat{\delta} = \delta_0$ but in practice, due to computational issues, the results can be off, depending on the metric. The results are shown in Fig. 5, where the left panel plots $\hat{\delta}$ versus δ_0 for a fixed signal, under the polynomial metric for different values of β . Depending upon β , this plot is close to the 45° line for small δ_0 but can deviate away for large δ_0 . In the right panel we fix $\delta_0 = 0.1$ and estimate it using $\hat{\delta}$ for a fixed β using different integration domains $(-\xi_0, \xi_0)$; the estimate $\hat{\delta}$ is plotted versus ξ_0 . Based on these experiments, we choose $\beta = 8$ for the later experiments.

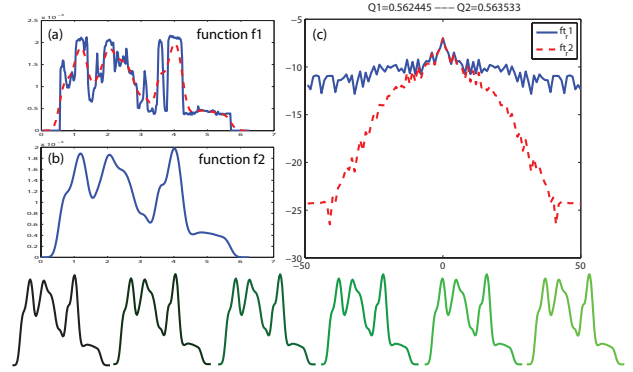


Figure 6. (a) The original function f_1 (b) blurred f_1 with $\delta_0 = 0.0025$, denote it f_2 and (c) \tilde{f}_1 and \tilde{f}_2 with $Q[\tilde{f}_1] = 0.562445$ and $Q[\tilde{f}_2] = 0.563533$. Bottom: The geodesic path between the log-Fourier representations of the two functions on the same section.

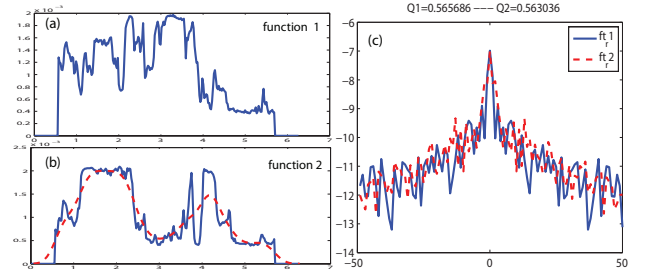


Figure 7. (a) f_1 (b) f_2 before and after smoothing and (c) \tilde{f}_1 and \tilde{f}_2 with $Q[\tilde{f}_1] = 0.565686$ and $Q[\tilde{f}_2] = 0.563036$. The estimated parameter is $\hat{\delta} = 0.0062$ and the resulting distance is 0.0692.

A single run of this experiment is shown in Fig. 6 where we take a signal f_1 (a), blur it using $\delta_0 = 0.0025$ to result in (b) and then apply the algorithm for estimating the blur level of f_1 to match f_2 . The algorithm estimates $\hat{\delta}$ to be 0.0025 and the resulting geodesic path between the $f_1 * K_{\hat{\delta}}$ and f_2 is shown in the bottom row. The resulting distance between the two signals is found to be insignificant $\sim 5 \times 10^{-7}$.

In the next experiment we compare two randomly selected signals f_1 and f_2 using the algorithm and the results are presented in Fig. 7. Here we compute the blur levels of the two functions $Q[\tilde{f}_1]$ and $Q[\tilde{f}_2]$ and use these values to estimate $\hat{\delta}$ needed to blur the function that has the smaller Q -value. After blurring using the estimated blur parameter, the two signals are now deemed to be at the same blur level and can be compared using the polynomial metric. The resulting distance between the two signals is the blur-invariant distance between them.

2D Image Comparisons: Without any significant modification, the theory presented here extends to 2D images, and we present some experimental results here without providing mathematical details. In the first experiment, we take

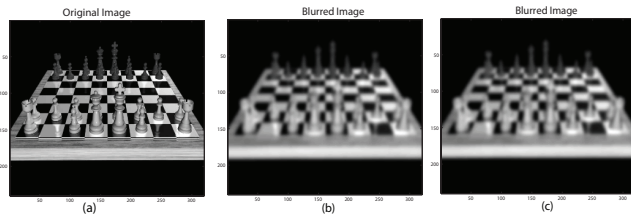


Figure 8. Example of blurring images (a) Original Image I_1 (b) $I_2 = I_1 * K_{\delta_0}$ with $\delta_0 = 0.81$; since $Q[\tilde{I}_1] = -2.1417$ and $Q[\tilde{I}_2] = 0.0730$, we get $\hat{\delta} = 0.81$. (c) $I_1 * K_{\hat{\delta}}$.



Figure 9. Each row shows two images (first,second) at different levels of blur. The one with lower Q -level is brought to the same level as the other and shown in (third). Then, the corresponding distances are computed. The resulting distances from top to bottom are: (1) 0.3238, (2) 0.2797, (3) 0.2734, (4) 0.27943.

an image shown in Fig. 8(a) and generate another image by blurring with a 2D Gaussian kernel with $\delta = 0.81$ Fig. 8(b). We then use their log-Fourier representations to compute Q levels and estimate the blur level $\hat{\delta}$ of I_1 , which is found to be exactly 0.81. Hence, the distance between them is 0.

In another experiment, we use several pairs of images and compute distances between them, as shown in Fig. 9. Since these images are taken from the same camera, and are at the same blur level, we intentionally blur one of the image by a certain amount. However, our method correctly estimates the δ , brings the two images at the same level, then compare the two images.

Fig. 10 shows a comparison of two distances: $\|I_1 * K_{\delta} - I_2 * K_{\delta}\|$ and the proposed distance $d(I_1 * K_{\delta}, I_2 * K_{\delta})$, versus δ for two left images shown in the bottom row of Fig.

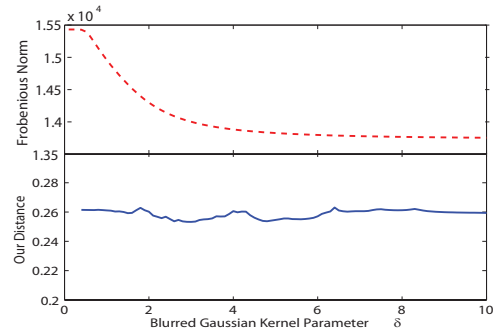


Figure 10. Variation of (a) $\|I_1 * K_{\delta} - I_2 * K_{\delta}\|$ and the proposed distance (b) $d(I_1 * K_{\delta}, I_2 * K_{\delta})$, versus δ , for I_1, I_2 shown in the bottom row of Fig. 9.

9. This is an experimental validation of the earlier theorem about the blurring action being by isometries.

5. Summary

We have introduced a log-Euclidean representation of images and signals, that together with a polynomial or an exponential metric, provides a blurring-invariant comparison of images. In this framework, one computes the blur levels of two images to be compared, and blurs the least blurred image to match the other. Once they are at the same level, we can compute a simple distance between them. This theoretical framework is demonstrated with several illustrative examples involving signals and images.

References

- [1] B. Bascle, A. Blake, and A. Zisserman. Motion deblurring and super-resolution from an image sequence. In *ECCV*, pages 573–582, 1996. 1
- [2] J. Flusser, T. Suk, and S. Saic. Recognition of blurred images by the methods of moments. *IEEE Transactions on Image Processing*, 5(3), 1996. 1
- [3] N. Joshi, C. L. Zitnick, R. Szeliski, and D. J. Kriegman. Image deblurring and denoising using color priors. In *CVPR*, 2009. 1
- [4] D. Kundur and D. Hatzinakos. Blind image deconvolution. *IEEE Signal Processing Magazine*, 13(3):43–64, 1996. 1
- [5] A. Levin, Y. Weiss, F. Durand, and W. T. Freeman. Understanding and evaluating blind deconvolution algorithms. In *Computer Vision and Pattern Recognition*, pages 1964–1971, 2009. 1
- [6] Y. Lu, J. Sun, L. Quan, and H.-Y. Shum. Image deblurring with blurred/noisy image pairs. *ACM Trans. on Graphics*, 26(3):1–10, 2007. 1
- [7] J. Portilla, M. Wainwright, and E. P. Simoncelli. Image denoising using scale mixtures of gaussians in the wavelet domain. *IEEE Trans. on Image Processing*, 12(11):1338–1351, 2003. 1
- [8] F. J. Sorel Michal, Sroubek Filip. Multichannel image deblurring of digital images. *Kybernetika*, 47(3):439–454, 2011. 1